www.czasopisma.pan.pl PAN POLSKA AKADEMIA NAUK www.journals.pan.pl

ARCHIVES OF ACOUSTICS
Vol. **45**, No. 2, pp. 349–357 (2020)
DOI: 10.24425/aoa.2020.133155

Research Paper

Underwater Noises of Open-Circuit Scuba Diver

Vladimir KORENBAUM[(1)*], Anatoly KOSTIV[(1)], Sergey GOROVOY[(1),(2)]
Veniamin DOROZHKO[(1)], Anton SHIRYAEV[(1)]

[(1)] *V.I. Il'ichev Pacific Oceanological Institute, Far Eastern Branch Russian Academy of Sciences*
Baltiyskaya 43, Vladivostook, 690041, Russia
[*]Corresponding Author e-mail: v-kor@poi.dvo.ru

[(2)] *Engineering School, Far Eastern Federal University*
Sukhanova 8, Vladivostok, 690090, Russia; e-mail: gorovoysv@mail.ru

(*received July 3, 2019; accepted January 21, 2020*)

The features of respiratory noises and noises of fins for open-circuit scuba divers, indicating a multipole character of noises emission, are specified in cameral conditions. It demonstrates a possibility to detect low-frequency components of noises of fins with pressure gradient sensor in near field. A possibility of estimating the respiratory rate of an open-circuit scuba diver is demonstrated at distances up to 100 m in real sea. It gives an opportunity of estimating the bearing (time delay in a pair of hydrophones) for the open-circuit scuba diver by respiratory noises at distances up to 150 m in real sea. Thus, low-frequency underwater noises of open-circuit scuba divers may be successfully applied to monitor the safety of diving and to prevent waterside intrusion by trespassers.

Keywords: underwater acoustics; diver; respiratory noises; noises of fins; open-circuit scuba; breathing apparatus; detection; monitoring; bearing.

1. Introduction

Passive acoustic monitoring of scuba divers is a promising way to monitor the safety of diving and to prevent waterside intrusion by trespassers. Respiratory noises and noises of fins emitted by a scuba diver into water may be applicable here.

The respiratory noises of an open-circuit scuba diver consist of the noise of exhaled and floating air bubbles (Lohrasbipeydeh *et al.*, 2014; Gorovoy *et al.*, 2014; Korenbaum *et al.*, 2016), while in inspiration the noises are connected to an operation of the high-pressure regulator in scuba breathing apparatus (Donskoy *et al.*, 2008; Gemba *et al.* 2014). These powerful quasi-periodic signals have a repetition frequency corresponding to diver's respiratory rate. Noises of fins are associated with hydrodynamic vortices created during their oscillatory movements.

Objective of the paper is detailed experimental study of low-frequency noises of an open-circuit scuba diver, emitted into water, and drafting possible applications.

2. Theory

The main sources of scuba diver noises have small wave size in low frequencies, and can be considered as the point multipole emitters. It is known that a point source of sound can oscillate with various modes, the main of them are monopole, dipole, and quadrupole.

The source of respiratory noises seems to be closer to monopole one. For a monopole source in an unlimited medium expressions for sound pressure

$$p = \frac{P_0 \exp(-ikr)}{r},$$

and radial component of oscillatory velocity

$$v_r = \frac{P_0 \exp(-ikr)}{\rho c r}\left(1 - \frac{i}{kr}\right)$$

are well known (Skouchek, 1976), where r – distance, P_0 – sound pressure at the distance of 1 m from the source, k – wavenumber, i – imaginary unit, c – sound speed in medium, ρ – its density. For this type of

source, the sound pressure in the unlimited space decreases in accordance with the $1/r$ law whereas the radial component of vibrational velocity decreases according to the $1/r^2$ law. The latter (non-wave) component dominates in the near field of the source, and approximately describes the hydrodynamic effect of the source on the point receiving sensor. An acoustic sensor in the form of omnidirectional pressure receiver (hydrophone) is weakly sensitive to such effect (Korenbum, Tagiltsev, 2012). Therefore, it is possible to measure the monopole source characteristics in its vicinity with hydrophones. On the contrary, vector sensors, in particular, made in the form of pressure gradient receivers, perceive the non-wave field component more efficiently than the wave one. The response of modern pressure gradient sensors is proportional to oscillatory acceleration

$$v_r' = i\omega \frac{P_0 \exp(-ikr)}{\rho c r}\left(1 - \frac{i}{kr}\right).$$

Obviously, it is more efficient to receive a signal for small kr, using pressure gradient sensors, whereas for large kr the potentials of pressure gradient sensor and pressure sensor are equalized by the signal due to attenuation of the non-wave component. A transition zone where an equality is achieved at $kr = 1$. For example, if you set the frequencies of the noise spectrum as 10–20 Hz, then at distances less than r = 24–12 m, a pressure gradient sensor should be more suitable for signal registration than a pressure sensor.

As for noises of fins, a fin movement is characterized by oscillations of its edge with a flow shedding, which can be represented as a dipole source. In the case of dipole source, its emission is given by sound pressure

$$p = B\frac{\exp(-ikr)}{r}\left(1 - \frac{i}{kr}\right)\cos\varphi,$$

and components of oscillatory velocity:

- radial

$$v_r = B\frac{\exp(-ikr)}{\rho c r}\left(1 - \frac{2i}{kr} - \frac{2}{(kr)^2}\right)\cos\varphi,$$

- and tangential

$$v_\tau = B\frac{\exp(-ikr)}{\rho c r^2}\left(1 - \frac{i}{kr}\right)\sin\varphi,$$

where B – constant of dipole emission (Skouchek, 1976). The tangential component of oscillatory velocity is an important feature of the near-field emission of the dipole source in comparison with the monopole one. In the far field an efficiency of dipole source emission is small compared to the monopole one. However, in the near field the dipole source radiates much more efficiently than the monopole one due to the existence of components proportional to $1/r^2$ (by sound pressure), $1/r^3$ (by radial component of oscillatory velocity), and $1/r^3$ (by tangential component of oscillatory velocity). This effect is physically explained by appearance of alternating hydrodynamic flows near the oscillating (dipole) source. It is obvious that likely to the case of monopole source a transition zone for effective reception by pressure gradient sensor is defined as $kr = 1$. Furthermore, an application of pressure gradient sensor to record emission of the components of oscillatory velocity (acceleration) of a dipole source in near-field zone seems to be even more advantageous than in a case of monopole source.

If we consider the radiation of a pair of fins in their alternate motion (swimming in the crawl style), then a second dipole emitter should be added to the first, turned on in invert phase at a distance of less than 0.25 m. The physical picture of alternating vertical oscillation of two fins looks like a so-called transverse quadrupole source. Its radiation similarly is given by sound pressure, radial and tangential components of oscillatory velocity (Skouchek, 1976). The emission efficiency of a quadrupole source in the far field is even lower than that of the dipole source. However, in the near field of such source the registering of components of oscillatory velocity (acceleration) by means of pressure gradient sensor may be even more beneficial than for dipole due to existence of components proportional to $1/r^3$ (by sound pressure), $1/r^4$ (by radial component of oscillatory velocity), and $1/r^4$ (by tangential component of oscillatory velocity).

3. Materials and methods

The hydroacoustic array was developed for experiments and consisted of 12 undirectional hydrophones distanced at 4 m. Each hydrophone was made in the form of an assembly of 3 standard piezoelectric cylinders of 18 mm diameter, sealed with common rubber sheath (Bogorodskiy *et al.*, 1983). To reduce the influence of hydrodynamic noise caused by water flows, sound-transparent fabric covers made of synthetic terry cloth 5 mm thick were put on each hydrophone. Hydrophones were connected to underwater electric cable with longitudinal sealing having total length of 100 m, on the remote part of which 12 hermetic taps were spaced apart at a distance of 4 m. Tap length was 3 m. The sealed containers were installed at the ends of the taps, which were connected to 2-wire hydrophone pins. Preamplifiers (gain 12) were installed inside containers. According to the results of calibration, the sensitivities of hydrophones (without preamplifiers) were between 100 and 154 μV/Pa. Additional amplification (gain 200) was applied before recording.

Additionally 3-component pressure gradient sensor of inertial type was used (Korenbaum *et al.*, 2017). It consisted of common foam housing and 3 orthogonally oriented accelerometers PCB 393B05 (Piezotronics) sealed into it. The sensitivity of every pressure gradient component to sound pressure in the flat wave was

near 500 μV/Pa at 100 Hz. Additional amplification was not applied. The housing was suspended with rubber files into sound-transparent grid metal case with heavy base. The case was covered with lattice synthetic cloth to reduce influence of hydrodynamic noise caused by water flows.

The signals were preconditioned, transmitted through electric cable, amplified and registered with 16-channel PowerLab (ADInstruments) recorder, sampling frequency of 10 kHz. FFT spectral analysis was performed with SpectraPLUS (Pioner Hill Software) software. Spectrograms were evaluated. The cross-correlation function and cross-correlograms of responses of pairs of hydrophones were calculated with specially designed software.

The respiratory noises of an open-circuit scuba diver were initially studied in the hydroacoustic basin. The scuba diver was placed in the center of the basin at rest. The hydrophones of array were placed at the bottom of the basin equally distanced at 1.2 m.

In real sea noises of open circuit scuba divers were recorded during wet shallow-water submersions in the Peter the Great Bay with dive depth of about 7–8 m. Noises were registered by the bottom-mounted (near 10 m) linear array of hydrophones equally distanced at 4 m and one 3-component pressure gradient sensor bottom-mounted near the hydrophone 2 of array (left about 0.5 m from its line).

The scuba diver displacement inside water area was monitored with GPS-tracker placed in airtight buoy, towed behind the diver with 8–10 m hawser at sea surface. To assess positions of hydrophones the diver, equipped with GPS-tracker, lay at the bottom consistently near each hydrophone of the array for several minutes. The diver had also a stop near the pressure gradient sensor.

4. Results and discussion

4.1. Respiratory noises of open-circuit scuba diver in the basin registered in near-field conditions with hydrophones

The open-circuit scuba diver was placed in the center of the basin at rest (without movement of fins). Spectrograms (8192 time samples, Hann window, 50% overlap) of responses of two bottom mounted hydrophones were analysed (Fig. 1).

The powerful respiratory signals are seen in both hydrophones (Fig. 1). Their repetition frequency corresponds to diver's respiratory rate, recognized by ear.

The beginning of exhalation is seen (Fig. 1 – *1*) in the frequency band of 70–130 Hz. It may be treated as a detachment of exhaled air bubble from the scuba apparatus. The main broadband signal of exhalation in the frequency band of 200–1000 Hz (Fig. 1 – *2*) starts a little later. Therefore, it may be connected to the noise of floating bubbles during expiration.

One can see especially in the frequency band of 70–130 Hz a noticeable widening of the low-frequency signal spectrum near the source of emission at the distance of 3 m (Fig. 1 – *1*, Right ch.) in comparison with the distance of 10 m (Fig. 1 – *1*, Left ch.). This may be explained by predicted above exposure of the hydrophones by near-field components of emission from complex source of respiratory noise. It looks like that not only pulsating but also higher components (dipole, quadropole) appear in the source at small wave distances. Thus, the source of low-frequency respiratory noises of open-circuit scuba diver could not be considered as a pure monopole as it was expected above.

The high-frequency signal in the frequency band of 2.5–4.9 kHz (Fig. 1 – *3*) may be associated with inspi-

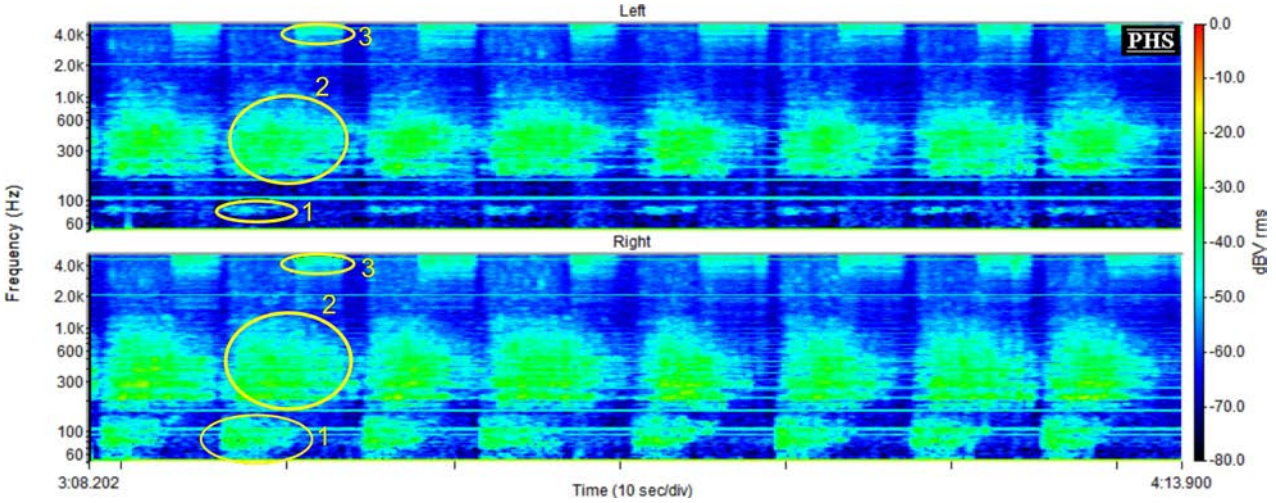

Fig. 1. Spectrograms of responses of hydrophones, placed in the basin near breathing open-circuit scuba diver – upper diagram (Left ch.) is a response of the hydrophone at distance of 10 m; bottom diagram (Right ch.) is a response of the hydrophone at distance of 3 m: *1* – noise in beginning of exhalation, *2* – noise of the main part of exhalation, *3* – high-frequency noise of inhalation.

ratory noises connected to an operation of the high-pressure regulator (Donskoy *et al.*, 2008; Gemba *et al.*, 2014).

4.2. Noises of fins and respiratory noises registered in near-field conditions with hydrophone and pressure gradient sensor

In order to record respiratory noises and noises of fins simultaneously, the open-circuit scuba diver in shallow-water area made a passage along the linear antenna array installed at the bottom (10 m) at a height of about 2 m above it. The spectrograms for this maneuver are shown in Fig. 2. The scheme of location and mutual orientation of pressure gradient components and the diver is shown in Fig. 3 (position of the diver when approaching pressure gradient sensor is indicated by *L1*, while moving away – *L2*). The diver moved from the hydrophone 1 to the hydrophone 12, i.e. his displacement coincided with the direction from right to left for Figs 2 and 3. The responses of the hydrophone 2 of the array and adjacent 3-component pressure gradient sensor to the passage of the diver are presented in Fig. 2.

The spectrogram of hydrophone 2 (Fig. 2a) in the frequency range of 40–400 Hz has typical vertical strips of respiratory noises (Fig. 2 – *1*) with a repetition frequency of about 0.2 Hz. The noises, as expected, reach a maximum of intensity (and maximum bandwidth expansion in the low-frequency range) when the diver passed directly above the hydrophone 2 (Fig. 2 – *1*). The range of detection of these noises (taking into account the speed of the diver about 0.5 m/s) is about 20 m, both approaching the hydrophone and distan-

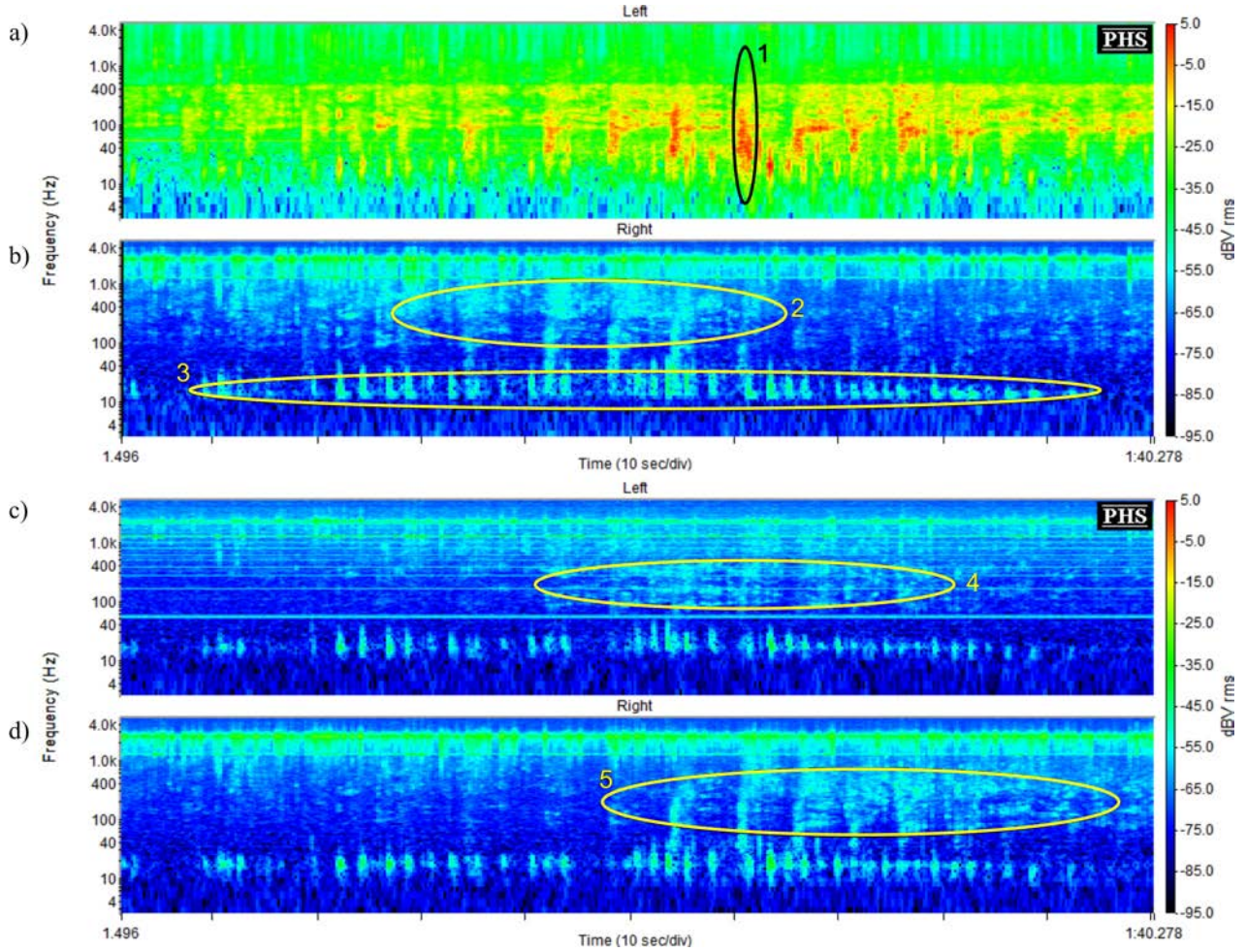

Fig. 2. Spectrograms of responses of bottom-mounted hydrophone 2 of the array and adjacent 3-component pressure gradient sensor to the scuba diver passage with fins (approximate velocity of 0.5 m/s) along the line of array at 2 m height above sensors: a) the hydrophone 2 of array; b) the pressure gradient component of longitudinal orientation, set at the angle of 45° from the bottom (Fig. 3 – *5*); c) the pressure gradient component of horizontal transverse orientation to the line of array; d) the pressure gradient component of longitudinal orientation, set at the angle of 135° from the bottom (Fig. 3 – *6*); *1* – fragment of respiratory noises of the hydrophone 2; *2* – fragment of respiratory noises of pressure gradient component of longitudinal orientation, set at the angle of 45° from the bottom; *3* – fragment of noises of fins; *4* – fragment of respiratory noises of pressure gradient component of transverse orientation; *5* – fragment of respiratory noises of pressure gradient component of longitudinal orientation, set at the angle of 135° from the bottom.

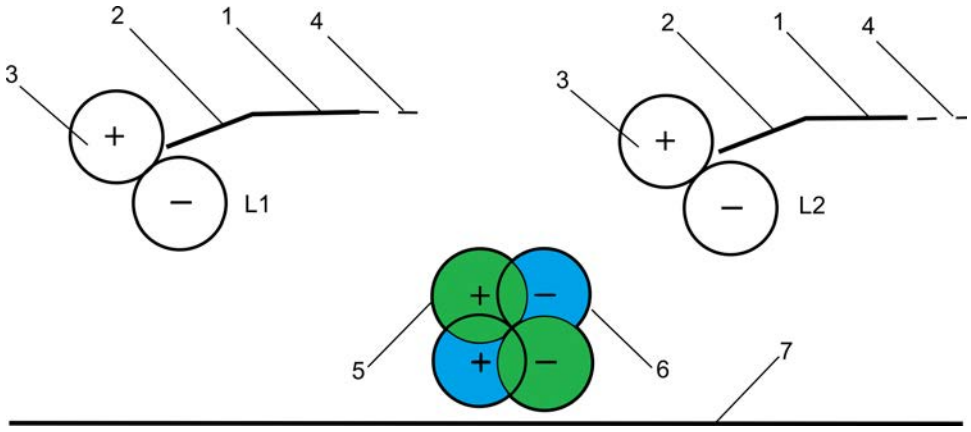

Fig. 3. Scheme of mutual orientation of the source of emission of fins of the diver with orientations of the pressure gradient sensor components: *L1* – position of the diver approaching the sensors, *L2* – position of the diver leaving the sensors, *1* – position of the leg of the diver, *2* – position of one fin, *3* – dipole component of emission of noises of the fin, *4* – direction of movement of the diver, *5*, *6* – dipole directivity patterns of pressure gradient components oriented longitudinally in relation to the line of movement of the diver and the line of the bottom antenna array (dipole directivity pattern of the pressure gradient component having transverse orientation is not shown), *7* – bottom of the water area.

cing from it. It should be noted that the signal re-reflection from the water surface can be neglected for distances up to the depth of the site (10 m) due to spherical divergence of the wave front. However, at larger distances a contribution of waveguide effects to the observed picture may not be excluded.

In the spectrogram (Fig. 2b) of the pressure gradient component, longitudinally oriented along the array line and installed at the angle of 45° from the bottom (Fig. 3 – *5*), respiratory noises are synchronous with the reply of the hydrophone 2, during approaching the sensors (Fig. 2 – *2*, Fig. 3 – *L1*). When the diver is passing over the pressure gradient sensor, which time is determined by the maximum of signals in the response of hydrophone 2 (Fig. 2 – *1*), and moving further away from gradient sensor (Fig. 3 – *L2*), these signals are significantly weakened. It may be explained by the dipole directivity of this pressure gradient component (Fig. 3 – *5*) oriented by its minimum to the source of respiratory noises. In the area of 2.5–3 kHz a continuous horizontal strip is seen in the spectrogram Fig. 2b. It is associated with the resonance of accelerometer.

Additionally, in the response of this pressure gradient component the more frequently repeated vertical strips are clearly visible in the frequency range of 10–30 Hz (Fig 2 – *3*), having a repetition frequency of about 0.5 Hz. It is interesting that similar formations are also seen in the spectrogram of hydrophone No. 2 (Fig. 2a) but less clearly. As the bandwidth of these spectral strips evidently increases when approaching pressure gradient sensor (Fig. 2b), they can be attributed to a noise associated with the movement of fins.

When the diver is passing over pressure gradient sensor and leaving it, the bandwidth of these spectral strips gradually decreases again. This probably may be connected with the specified vertical orientation of a dipole component of the source (Fig. 3 – *L2, 3*) to the sensor (Fig. 3 – *5*). The range of detection of these noises when approaching pressure gradient sensor is about 25 m, and when departing it – 17 m. It is worth noting that the distances are close to the above mentioned theoretically predicted estimates for $kr = 1$ in frequency range of 10–20 Hz.

In the spectrogram (Fig. 2c) of the pressure gradient component oriented horizontally in transverse direction to the array line, and by minimum of its directivity pattern to the route of the diver, respiratory associated noises are observed only when the diver is passing above the sensor. Moreover the signals are significantly weakened (Fig. 2 – *4*). The characteristic spectral strips of respiratory noise are blurred (especially below 500 Hz). It is interesting that an asymmetry between ranges of detecting respiratory noises of the diver during approaching the sensor and distancing from it disappears in this case. The observed effects can be associated with the predominant registering not radial but tangential component of oscillatory acceleration of the respiratory noise source, which confirms its multipole character (a presence of the dipole and quadrupole components described above) in the near field. This speculation is confirmed by almost as stable registration of noises associated with movement of fins, as for the longitudinally oriented component of pressure gradient sensor (Fig. 2 – *3*). As noises of fins lie in the lower frequency region (below 20–30 Hz) than the main respiratory noises, this effect is even more pronounced here and makes it possible to detect these noises at practically the same distances that were found for the longitudinally oriented pressure gradient component (Fig. 2b) and had been theoretically predicted for $kr = 1$.

In the spectrogram (Fig. 2d) of the longitudinally oriented pressure gradient component, installed at the angle of 135° from the bottom (Fig. 3 – *6*), a mirror image is seen with respect to the longitudinal component of pressure gradient sensor (Fig. 2b) oriented orthogonally to it (Fig. 3 – *5*) in terms of respiratory noises. Here the respiratory noises are amplified when the diver is moving from the sensor. The effect may be connected to the mirror orientations of the dipole directivity patterns of pressure gradient components under consideration (Fig. 3 – *6 vs* Fig. 3 – *5*) manifesting for far field ($kr < 1$). Whereas the noises associated with fins are visible almost at the same distances and with characteristics similar in frequency bands to other pressure gradient components. This observation may be interpreted in favour of the predominantly near-field ($kr < 1$) character of emission of recorded noises of fins by the dipole/quadrupole sources. A combination of these sources has in near field predicted above tangential emission components leading to a loss of the dipole directivity typical for the pressure gradient sensor components in far field.

4.3. Detection of open-circuit scuba diver by respiratory noises in real sea and estimation of acoustic bearing

Respiratory sounds of open-circuit scuba divers were recorded in summer during shallow-water submersions in the Peter the Great Bay, Japan Sea near port of Vladivostok with dive depth of about 7–8 m (sea state 2–3 on the Beaufort scale; sandy bottom with a depth of around 10 m). A high level of external background noise was observed during the experiment, that included intensive continuous and discrete spectral components of noise of many small boats as well as intensive pulse noise components generated by marine crustaceans. The averaged spectral levels of sea noise during trials corresponded to the (Wentz, 1962) curves for deep sea with a sea state up to 7 on the Beaufort scale.

Noises were registered with described (Subsec. 4.2) bottom-mounted array of hydrophones. The open-circuit scuba diver moved with fins away from the hydrophone 2. Spectrogram (8192 time samples, Hann window, 50% overlap) for the hydrophone 2 is shown in Fig. 4. Respiratory noises of the diver are visible in the frequency range of 30–1000 Hz in vicinity of the hydrophone with progressive narrowing of this band to about 100–300 Hz when the distance from the hydrophone is increasing (Fig. 4). The vertical strips of respiratory noises are seen in the spectrogram during at least 200 s. Since velocity of the diver displacement was around 0.5 m/s maximal distance of his detection in the spectrogram may be assessed as 100 m. In accordance with the basin measurements (Subsec. 4.1) the vertical strips in the spectrogram should mostly characterize the noise of floating bubbles during expiration. The signals provide a possibility to estimate the diver's respiratory rate being about 0.25 Hz for this fragment (Fig. 4) and may be applied for passive detection and bearing estimation.

It should be noted that inspiratory high-frequency noises are not identified clearly here in contrast with the basin measurements (Subsec. 4.1). This probably may be explained by specific hydrology or bottom properties. The low-frequency noises of fins recorded in near field conditions (Subsec. 4.2) are visible here only close to the hydrophone. The latter seems to be caused by the waveguide effects, neglected at small distances in the Subsec. 4.2.

Previously only high-frequency (above 1 kHz) part of respiratory noises was used for bearing estimation of open-circuit scuba divers (Sutin *et al.*, 2013). However, it is evident that low-frequency acoustic signs (Fig. 4) may also provide monitoring of the displacement of a scuba diver by means of determining the time delays of maxima of cross-correlation function at

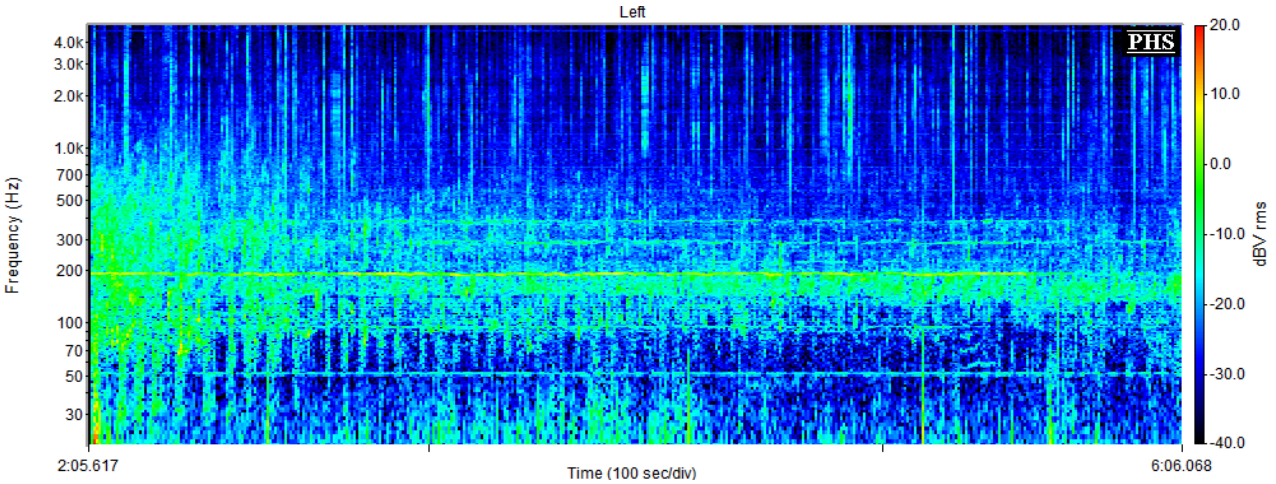

Fig. 4. Spectrogram of response of the bottom-mounted hydrophone 2 to open-circuit scuba diver passage with fins away from the hydrophone (velocity of about 0.5 m/s).

two hydrophones. The time delay may be used to assess the acoustic bearing in well-known manner. An example of the trace of such time delays for the pair of hydrophones is shown in the correlograms of normalized cross-correlation function R_{xy} (Fig. 5). The correlograms are evaluated for approximately the same time fragment which spectrogram is shown in Fig. 4. The raw correlogram with time accumulation 1 s (50% overlap) is represented in Fig. 5a. The correlogram with automatically found maxima of normalized correlation function in each interval of accumulation (highlighted with red dots) is seen in Fig. 5b.

The distance between geometric center of pair of hydrophones 2 and 7, and the buoy with GPS-tracker towed by the diver in this maneuver is shown in Fig. 6.

Time delays of automatically found maxima of normalized cross-correlation function R_{xy} and time delays calculated by GPS data as well as the value of normalized cross-correlation function R_{xy} for this maneuver are shown in Fig. 7.

In correlogram Fig. 5a one can see the trace of maxima of normalized cross-correlation function during all analyzed fragment from 13:39 up to 13:44 of local time. In this time fragment the distance between diver (towered buoy) and the center point on the line connecting pair of hydrophones 2 and 7 changed from about 20 m up to 150 m (Fig. 6). The trace (Fig. 5a) has maximum amplitudes and minimal width in the vicinity of hydrophones and decreases gradually with increasing the distance. However, at the end of the time fragment

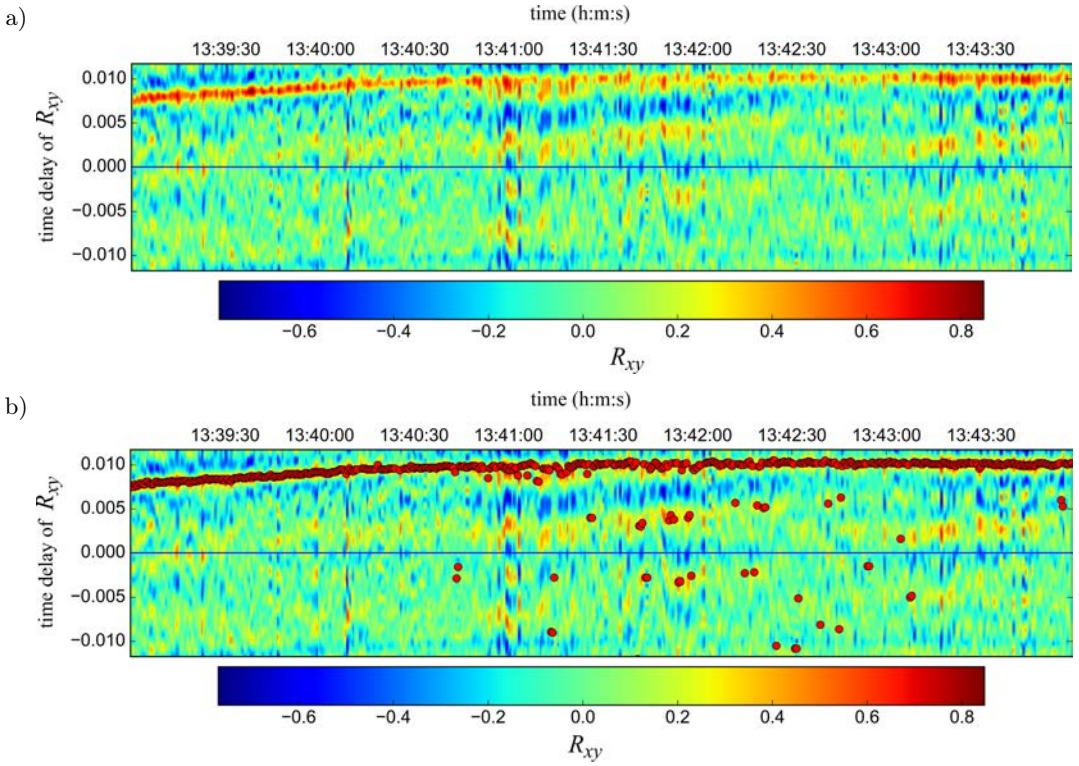

Fig. 5. a) Correlograms of responses of hydrophones 2 and 7 (distanced at 20 m) of the array to underwater noise during movement of the open-circuit scuba diver away from the pair of hydrophones approximately along the axis between hydrophones on local time of the day – raw correlogram; b) correlogram with automatically found maxima of normalized correlation function in each interval of accumulation (red dots).

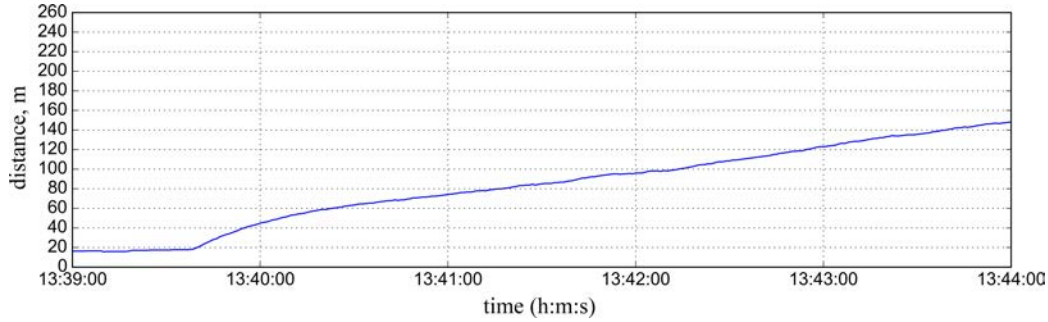

Fig. 6. GPS distance between the diver (towed buoy) and the center point of the pair of hydrophones 2, 7 as a dependence on local time of the day.

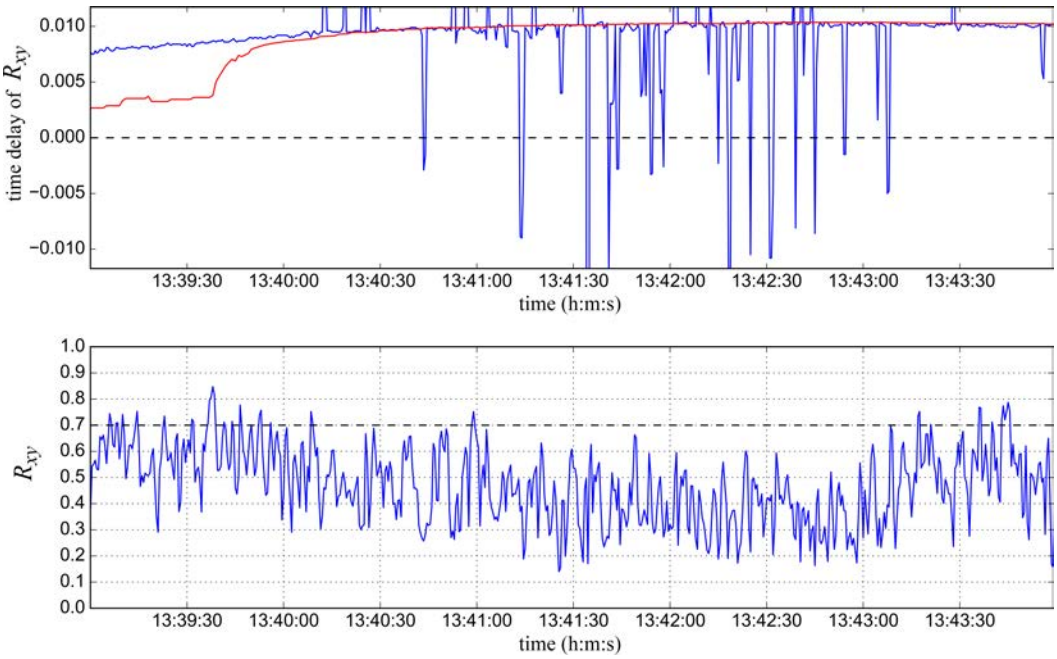

Fig. 7. Time delays of maxima of cross-correlation function (blue) with time delays calculated by GPS data (red) – upper diagram; and the value of coefficient of normalized cross-correlation function R_{xy}as a dependence on local time of the day – bottom diagram.

an amplification of the amplitudes of the trace is observed again. This unusual behaviour may probably be explained by changing in hydrology or bottom properties along the diver route. Moreover in the correlogram Fig. 5a additional and more fuzzy traces are seen for other noise sources.

Additional procedure of calculating maxima of normalized cross-correlation function in each time interval forms the correlogram with automatically found maxima labelled with red dots (Fig. 5b). These automatically found dots are used to evaluate acoustic time delays for the upper diagram in Fig. 7 and R_{xy} meanings for the bottom diagram in Fig. 7.

In the whole analyzed time fragment the values of maxima of normalized cross-correlation function R_{xy} of two hydrophones are between 0.4–0.6 (Fig. 7, bottom diagram). Meanwhile they were no more than 0.3 under background noises.

One can see (Fig. 7, upper diagram) that acoustic and GPS time delays (both determining bearing) are aligned near a distance of 45 m being in common very close to each other up to the distance of about 150 m.

However, there are several failures in the evaluation of acoustic time delays especially between 13:41 and 13:43 of local time. An origin of these failures is probably connected to additional more fuzzy traces in the correlogam Fig. 5a for which a number of false found dots is automatically calculated in the correlogram Fig. 5b for the same time fragment. Probably some kind of smoothing technique should be used to fend off these failures in future.

Another problem is a mismatch of acoustic and GPS time delays at short distances up to 45 m. This problem is connected to an incorrectness of calculation of acoustic time delay because the range between hydrophones (20 m) is of the same order as the distance to the diver here. Thus the necessary condition of a locally flat wave is not satisfied for both hydrophones at small distances.

Nevertheless for large distances (far above between-hydrophones range) the traces of time delays in correlograms (like in Fig. 5) are quite accurate (Fig. 7, upper diagram) and should provide a possibility of the triangulation estimate of the diver location with several pairs of hydrophones. It will be the topic for future study.

5. Conclusions

The features of respiratory noises and noises of fins for open-circuit scuba divers, indicating the multipole character of emission are specified. A possibility to detect low-frequency components of noises of fins with pressure gradient sensor is demonstrated. An opportunity of estimating the respiratory rate of an open-circuit scuba diver by his respiratory noises is demonstrated at distances up to 100 m in real sea. It shows a possibility of estimating the bearing (time delay in a pair of hydrophones) for the open-circuit scuba diver by respiratory noises at distances up to 150 m in real sea.

The results suggest that low-frequency underwater noises of open-circuit scuba divers may be successfully applied to monitor the safety of diving activity and to prevent waterside intrusion by trespassers.

Acknowledgements

The study was supported by the Program of Basic Research of the Russian Academy of Sciences (Project No. 0271-2019-0010) and partially supported by the Program of the Russian Academy of Sciences "New challenges of Earth climate system" (State reg. No. AAAA-A20-120031890011-8).

References

1. Bogorodskiy V.V., Zubarev L.A., Korepin Ye.A., Yakushev V.I. (1983), *Underwater electroacoustic transducers. Manual* [in Russian], Sudostroyeniye, St. Petersburg, pp. 91.
2. Donskoy D., Sedunov N., Tsionskiy M. (2008), Variability of SCUBA diver's acoustic emission, *Proceedings of SPIE, Optics and Photonics in Global Homeland Security IV*, C.S. Halvorson, D. Lehrfeld, T.T. Saito [Eds], **6945**, 694515–694515–11, doi: 10.1117/12.783500.
3. Gemba K.L., Nosal E.-M., Reed T.R. (2014), Partial dereverberation used to characterize open circuit scuba diver signatures, *Journal of Acoustic Society of America*, **136**(2): 623–633, doi: 10.1121/1.4884879.
4. Gorovoy S. *et al.* (2014), A possibility to use respiratory noises for diver detection and monitoring physiologic status, *Proceedings of Meetings on Acoustics (POMA)*, **21**: 070007, doi: 10.1121/1.4893767.
5. Korenbaum V.I., Tagiltsev A.A. (2012), Flow noise of an underwater vector sensor embedded in a flexible towed array, *Journal of Acoustic Society of America*, **131**(5): 3755–3762, doi: 10.1121/1.3693647.
6. Korenbaum V.I. *et al.* (2016), The possibility of passive acoustic monitoring of a scuba diver, *Doklady Earth Sciences*, **466**(2): 187–190, doi: 10.1134/S1028334X16020136.
7. Korenbaum V.I., Tagiltsev A.A., Gorovoi S.V., Kostiv A.E., Shiryaev A.D. (2017), Low-frequency inertial-type pressure-gradient receivers for oceanological investigations, *Instruments and Experimental Techniques*, **60**(4): 600–604, doi: 10.1134/S0020441217040066.
8. Lohrasbipeydeh H., Dakin T., Gulliver T.A., De Grasse C. (2014), Passive energy based acoustic signal analysis for diver detection, *Proceedings OCEANS 2014*, St John's, doi: 10.1109/OCEANS.2014.7003266.
9. Skouchek E. (1976), *Principles of Acoustics, Part 2* [in Russian], Mir, Moscow, pp. 105–133.
10. Sutin A., Salloum H., Delorme M., Sedunov N., Sedunov A., Tsionskiy M. (2013), Stevens passive acoustic system for surface and underwater threat detection, *IEEE International Conference on Technologies for Homeland Security, HST 2013*, art. no. 6698999, pp. 195–200, doi: 10.1109/THS.2013.6698999.
11. Wenz G.M. (1962), Acoustic ambient noise in the ocean: spectra and sources, *Journal of Acoustic Society of America*, **34**(12): 1936–1956, doi: 10.1121/1.1909155.